

Modeling Of Single-Phase To Three-Phase Drive System Using Two Parallel Single-Phase Rectifiers

Radha Krishna¹, Amar kiran²

^{1,2} (Department of EEE, GIET, JNTU University, Kakinada)

Abstract: This paper proposes a single-phase to three-phase drive system composed of two parallel single-phase rectifiers, a three-phase inverter, and an induction motor. The proposed topology permits to reduce the rectifier switch currents, the harmonic distortion at the input converter side, and presents improvements on the fault tolerance characteristics. Even with the increase in the number of switches, the total energy loss of the proposed system may be lower than that of a conventional one. The model of the system is derived, and it is shown that the reduction of circulating current is an important objective in the system design. A suitable control strategy, including the pulse width modulation technique (PWM), is developed. Experimental results are presented as well.

Index Terms—Ac-dc-ac power converter, drive system, parallel Converter, Fault Identification System (FIS).

I. INTRODUCTION

Several solutions have been proposed when the objective is to supply a three-phase motor from single-phase ac mains [1]-[4]. It is quite common to have only a single phase power grid in residential, commercial, manufacturing, and mainly in rural areas, while the adjustable speed drives may request a three-phase power grid. Single-phase to three-phase ac-dc-ac conversion usually employs a full-bridge topology, which implies in ten power switches. This converter is denoted here as conventional topology.

Parallel converters have been used to improve the power capability, reliability, efficiency, and redundancy. Parallel converter techniques can be employed to improve the performance of active power filters [5]-[6], uninterruptible power supplies (UPS) [7], fault tolerance of doubly fed induction generators, and three-phase drives [8]. Usually the operation of converters in parallel requires a transformer for isolation. However, weight, size, and cost associated with the transformer may make such a solution undesirable [9]. When an isolation transformer is not used, the reduction of circulating currents among different converter stages is an important objective in the system design [10]-[12].

In this paper, a single-phase to three-phase drive system composed of two parallel single-phase rectifiers and a three-phase inverter is proposed. The proposed system is conceived to operate where the single-phase utility grid is the unique option available. Compared to the conventional topology, the proposed system permits: to reduce the rectifier switch currents; the total harmonic distortion (THD) of the grid current with same switching frequency or the switching frequency with same THD of the grid current; and to increase the fault tolerance characteristics. In addition, the losses of the proposed system may be lower than that of the conventional counterpart. The aforementioned benefits justify the initial investment of the proposed system, due to the increase of number of switches.

II. METHODS TO CONNECT SINGLE PHASE TO THREE PHASE DRIVE SYSTEMS

2.1 Static Phase Converter:

Static Phase Converters operate by charging and discharging capacitors to temporarily produce a 3rd phase of power for only a matter of seconds during startup of electric motors, then it will drop out forcing the motor to continue to run on just 1 phase and only part of its windings. Due to their technology, Static Phase Converters do not properly power any class of 3 phase machinery or equipment. They will not in any way power 3 phase welders, 3 phase battery chargers, 3 phase lasers, or any type of machinery with 3 phase circuitry. Static Phase Converters also will not start delta wound 3 phase motors.

2.2 Rotary phase converter:

A rotary phase converter, abbreviated RPC, is an electrical machine that produces three-phase electric power from single-phase electric power. This allows three phase loads to run using generator or utility-supplied single-phase electric power. A rotary phase converter may be built as a motor-generator set. These have the advantage that in isolating the generated three-phase power from the single phase supply and balancing the three-phase output. However, due to weight, cost, and efficiency concerns, most RPCs are not built this way. Rotary Phase Converters Provide Reliable, Balanced, and Efficient Three Phase Power. Quick and Effective Three Phase Electricity.

All converters can be mainly categorized into two groups: one is cascade type and another is unified type [2]. In cascade type, the PWM converter for power factor correction and the PWM inverter for speed control are connected in series with large DC-Link capacitor and two static power converters are operated and controlled in separate. In this type, specific number of switches, to compose the converter and inverter, are required. Therefore, the required number of switches cannot be reduced significantly. On the other hand, in the unified type, conventional concepts of PWM converter and inverter are merged together and same converter handles the functions of PWM converter (power factor correction) and PWM inverter (motor control) at the same time. As an added advantage, the input inductor, which is commonly used in the PWM

converter for power factor correction, can be eliminated and replaced by the existing motor inductor. Therefore, this new concept can significantly reduce the number of components, compared to any conventional cascade type topologies.

III. SYSTEM MODEL

The Conventional system single-phase to three phase system and the Proposed system single phase to three phase systems are labeled as fig 1 and fig 2 respectively as shown below:

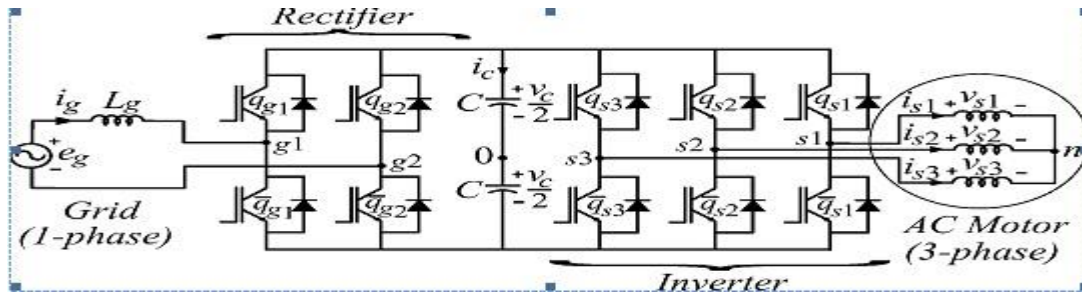


Fig 1 Conventional single-phase to three-phase system

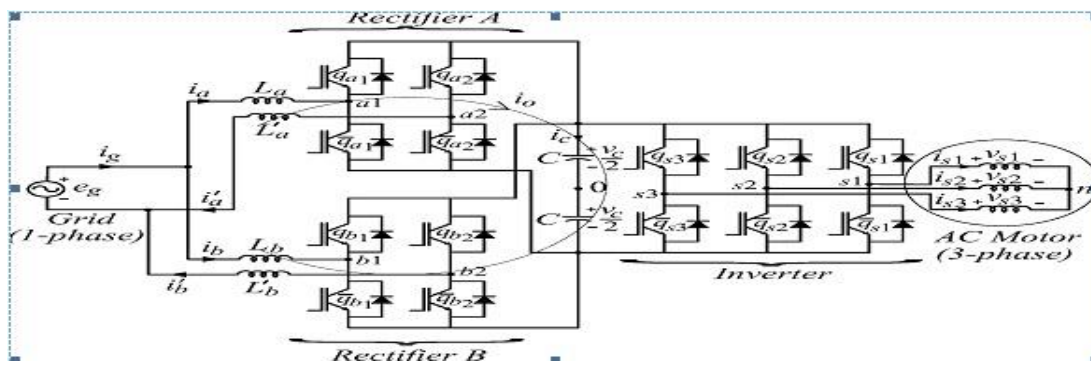


Fig 2 Proposed single-phase to three-phase drive system

The system is composed of grid, input inductors (L_a, L'_a, L_b, L'_b). Rectifiers (A and B), capacitor bank at the dc-link, inverter, and induction machine. Rectifiers A and B are constituted of switches $q_{a1}, \bar{q}_{a1}, q_{a2}$ and \bar{q}_{a2} and $q_{b1}, \bar{q}_{b1}, q_{b2}$ and \bar{q}_{b2} respectively. The inverter is constituted of switches $q_{s1}, \bar{q}_{s1}, q_{s2}, \bar{q}_{s2}, q_{s3}$ and \bar{q}_{s3} .

From Fig. 2, the following equations can be derived for the front-end rectifier

$$v_{a10} - v_{a20} = e_g - (r_a + l_a p)i_a - (r'_a + l'_a p)i'_a \quad (1)$$

$$v_{b10} - v_{b20} = e_g - (r_b + l_b p)i_b - (r'_b + l'_b p)i'_b \quad (2)$$

$$v_{a10} - v_{b10} = (r_b + l_b p)i_b - (r_a + l_a p)i_a \quad (3)$$

$$v_{a20} - v_{b20} = (r'_a + l'_a p)i'_a - (r'_b + l'_b p)i'_b \quad (4)$$

$$i_g = i_a + i_b = i'_a + i'_b \quad (5)$$

Where $p = d/dt$ and symbols like r and l represent the resistances and inductances of the input inductors L_a, L'_a, L_b, L'_b .

The circulating current i_0 can be defined from i_a, i'_a, i_b, i'_b .

$$i_0 = i_a - i'_a = -i_b + i'_b \quad (6)$$

Introducing i_0 and adding (3) and (4), relations (1)–(4) Become

$$v_a = e_g - [(r'_a + r'_a) + (l_a + l'_a)p]i_a + (r'_a + l'_a p)i_0 \quad (7)$$

$$v_b = e_g - [(r'_b + r'_b) + (l_b + l'_b)p]i_b + (r'_b + l'_b p)i_0 \quad (8)$$

$$v_0 = -[(r'_a + r'_b) + (l_b + l'_b)p]i_0 + [(r'_a - r'_a) + (l_a - l'_a)p]i_a + [(r'_b - r'_b) + (l_b + l'_b)p]i_b \quad (9)$$

$$\text{Where } v_a = v_{a10} - v_{a20} \quad (10)$$

$$v_b = v_{b10} - v_{b20} \quad (11)$$

$$v_0 = v_{a10} + v_{a20} - v_{b10} - v_{b20} \quad (12)$$

Relations (7)–(9) and (5) constitute the front-end rectifier dynamic model. Therefore, v_a (rectifier A), v_b (rectifier B), and v_0 (rectifiers A and B) are used to regulate currents i_a, i_b, i_0 respectively. Reference currents i_a^* and i_b^* are chosen equal to $i_g^*/2$ and the reference circulating current i_0^* is chosen equal to 0.

In order to both facilitate the control and share equally current, voltage, and power between the rectifiers, the four inductors should be equal, i.e., $r'_g = r'_a = r'_b$ and $l'_g = l_a = l'_a = l_b = l'_b$. In this case, the model (7)–(9) can be simplified to the model given by

$$v_a + \frac{v_0}{2} = e_g - 2(r'_g + l'_g p)i_a \quad (13)$$

$$v_a - \frac{v_0}{2} = e_g - 2(r'_g + l'_g p)i_b \quad (14)$$

$$v_0 = -2(r'_g + l'_g p)i_0 \quad (15)$$

Additionally, the equations for i_g, i'_a and i'_b can be written as

$$v_{ab} = \frac{v_a + v_b}{2} = e_g - (r'_g + l'_g p)i_g \quad (16)$$

$$v_a - \frac{v_0}{2} = e_g - 2(r'_g + l'_g p)i'_a \quad (17)$$

$$v_a + \frac{v_0}{2} = e_g - 2(r'_g + l'_g p)i'_b \quad (18)$$

In this ideal case (four identical inductors), the circulating current can be reduced to zero imposing.

$$v_0 = v_{a10} + v_{a20} - v_{b10} - v_{b20} = 0. \quad (19)$$

When $i_0 = 0$ ($i_a = i'_a, i_b = i'_b$) the system model (7)–(9) is reduced to

$$v_a = e_g - 2(r'_g + l'_g p)i_a \quad (20)$$

$$v_b = e_g - 2(r'_g + l'_g p)i_b \quad (21)$$

IV. PWM STRATEGY

The PWM strategy for the rectifier will be presented. The rectifier pole voltages $v_{a10}, v_{a20}, v_{b10}$ and v_{b20} depend on the conduction states of the power switches, i.e.,

$$v_{j0} = (2s_{qj} - 1) \frac{v_c}{2}, \text{ for } j = a1 \text{ to } b2 \quad (22)$$

Where v_c is the total dc-link voltage. Considering that v_a^*, v_b^* and v_0^* denote the reference voltages determined by the current controllers.

$$v_a^* = v_{a10}^* - v_{a20}^* \quad (23)$$

$$v_b^* = v_{b10}^* - v_{b20}^* \quad (24)$$

$$v_0^* = v_{a10}^* + v_{a20}^* - v_{b10}^* - v_{b20}^* \quad (25)$$

The gating signals are directly calculated from the reference pole voltages v_{a10}^* , v_{a20}^* , v_{b10}^* and v_{b20}^* . However, (23)–(25) are not sufficient to determine the four pole voltages uniquely from v_a^* , v_b^* and v_0^* . Introducing an auxiliary variable $v_x^* = v_{a20}^*$, that equation plus the three equations (23)–(25) constitute a four independent equations system with four variables (v_{a10}^* , v_{a20}^* , v_{b10}^* and v_{b20}^*). Solving this system of equations, we obtain

$$v_{a10}^* = v_a^* + v_x^* \tag{26}$$

$$v_{a20}^* = v_x^* \tag{27}$$

$$v_{b10}^* = \frac{v_a^*}{2} + \frac{v_b^*}{2} - \frac{v_0^*}{2} + v_x^* \tag{28}$$

$$v_{b20}^* = \frac{v_a^*}{2} - \frac{v_b^*}{2} - \frac{v_0^*}{2} + v_x^* \tag{29}$$

From these equations, it can be seen that, besides v_a^* , v_b^* and v_0^* , the pole voltages depend on also of v_x^* . The limit values of the variable v_x^* can be calculated by taking into account the maximum $v_c^*/2$ and minimum $-v_c^*/2$ value of the pole voltages.

$$v_{xmax}^* = \frac{v_c^*}{2} - v_{max}^* \tag{30}$$

$$v_{xmin}^* = \frac{v_c^*}{2} - v_{min}^* \tag{31}$$

Where v_c^* is the reference dc-link voltages, $v_{max}^* = \max \vartheta$ and $v_{min}^* = \min \vartheta$, with

$$\vartheta = \{ v_a^*, 0, v_a^*/2 + v_b^*/2 - v_0^*/2, v_a^*/2 - v_b^*/2 - v_0^*/2 \}. \text{Introducing a parameter } \mu \text{ (} 0 \leq \mu \leq 1 \text{), the variable } v_x^* \text{ can be}$$

written as

$$v_x^* = \mu v_{xmax}^* + (1 - \mu) v_{xmin}^* \tag{32}$$

When $\mu = 0$, $\mu = 0.5$, and $\mu = 1$ the auxiliary variable v_x^* has the following values $v_x^* = v_{xmin}^*$, $v_x^* = v_{xave}^* = (v_{xmin}^* + v_{xmax}^*)/2$ and $v_x^* = v_{xmax}^*$, respectively. When $v_x^* = v_{xmax}^*$ or $v_x^* = v_{xmin}^*$ a converter leg operates with zero switching frequency. The gating signals are obtained by comparing pole voltages with one (v_{t1}), two (v_{t1} and v_{t2}) or more high-frequency triangular carrier signals. In the case of double-carrier approach, the phase shift of the two triangular carrier signals (v_{t1} and v_{t2}) is 180° . The parameter μ changes the place of the voltage pulses related to v_a and v_b . When $v_x^* = v_{xmin}^*$ ($\mu = 0$) or $v_x^* = v_{xmax}^*$ ($\mu = 1$) are selected, the pulses are placed in the begin or in the end of the half period (T_s) of the triangular carrier signal. On the other hand, when $v_x^* = v_{xave}^*$ the pulses are centered in the half period of the carrier signal.

The change of the position of the voltage pulses leads also to the change in the distribution of the zero instantaneous voltages (i.e., $v_a = 0$ and $v_b = 0$). With $\mu = 0$ or $\mu = 1$ the zero instantaneous voltages are placed at the beginning or at the end of the switching period, respectively, while with $\mu = 0.5$, they are distributed equally at the beginning and at the end of the half period. This is similar to the distribution of the zero-voltage vector in the three-phase inverter.

V. CONTROL STRATEGY

The control block diagram of Fig 2 highlighting the control of the rectifier to control the dc-link voltage and to guarantee the grid power factor close to one. Additionally, the circulating current i_0 in the rectifier of the proposed system needs to be controlled is shown below:

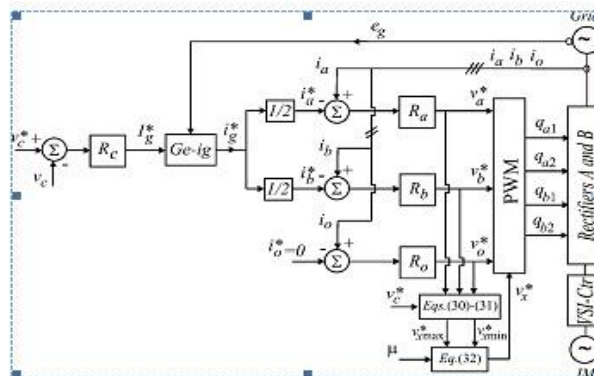


Fig 3 Control block diagram

In this way, the dc-link voltage v_c is adjusted to its reference value v_c^* using the controller R_c . Which is standard Fuzzy logic controllers. This controller provides the amplitude of the reference grid current i_g^* . To control power factor and harmonics in the grid side, the instantaneous reference current i_g^* must be synchronized with voltage e_g , as given in the voltage-oriented control (VOC) for three-phase system. This is obtained via blocks $Ge-i_g$, based on a PLL scheme. The reference currents i_a^* and i_b^* are obtained by making $i_a^* = i_b^* = i_g^*/2$. Which means that each rectifier receives half of the grid

current. The control of the rectifier currents is implemented using the controllers indicated by blocks R_a and R_b . These controllers can be implemented using linear or nonlinear techniques.

The homopolar current is measured (i_0) and compared to its reference ($i_0^* = 0$). The error is the input of Fuzzy controller R_0 , that determines the voltage v_0^* . The calculation of voltage v_0^* is given from (30) to (32) as a function of μ , selected. The motor three phase voltages are supplied from the inverter (VSI). Block VSI-Ctr indicates the inverter and its control. The control system is composed of the PWM command and a torque/flux control strategy.

VI. FAULT COMPENSATION

The proposed system presents redundancy of the rectifier converter, which can be useful in fault-tolerant systems. The proposed system can provide compensation for open-circuit and short-circuit failures occurring in the rectifier or inverter converter devices. The fault compensation is achieved by reconfiguring the power converter topology with the help of isolating devices (fast active fuses— $F_j, j = 1, \dots, 7$) and connecting devices (back to back connected SCRs— t_1, t_2, t_3), as observed in Fig. 10(a) and discussed. These devices are used to redefine the post-fault converter topology, which allows continuous operation of the drive after isolation of the faulty power switches in the converter. Fig. 7.8.1(b) presents the block diagram of the fault diagnosis system. In this figure, the block fault identification system (FIS) detects and locates the faulty switches, defining the leg to be isolated. This control system is based on the analysis of the pole voltage error. The fault detection and identification is carried out in four steps:

1. Measurement of pole voltages (v_{j0}).
2. Computation of the voltage error ϵ_{j0} by comparison of reference voltages and measurements affected in Step (1).
3. Determination as to whether these errors correspond or not to a faulty condition; this can be implemented by the hysteresis detector.
4. Identification of the faulty switches by using ϵ_{j0} .

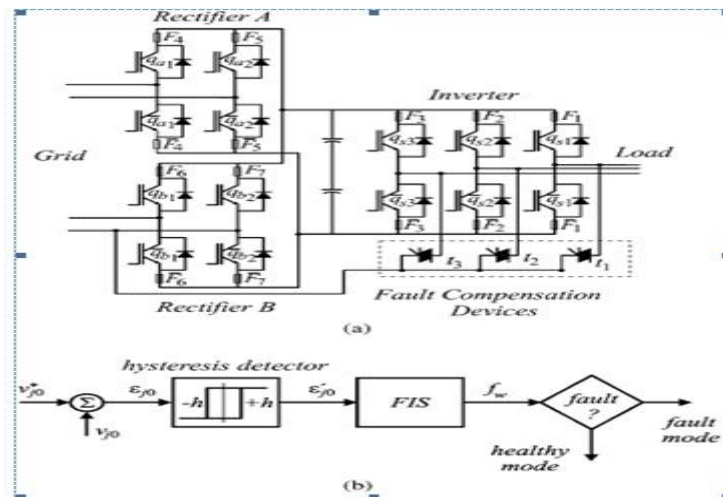


Fig.4 (a) Proposed configuration highlighting devices of fault-tolerant system.
 (b) Block diagram of the fault diagnosis system.

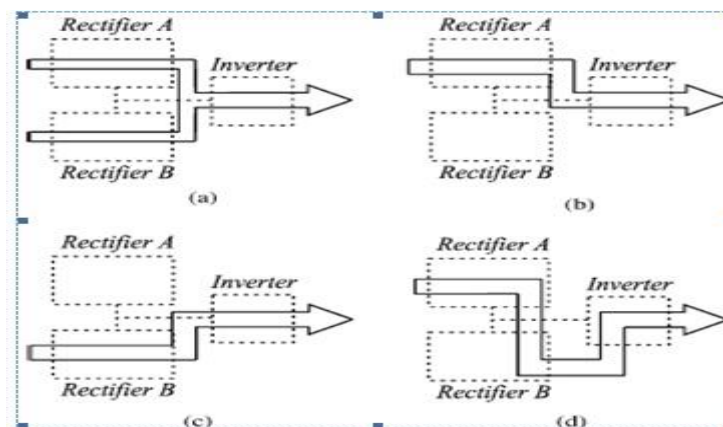


Fig.5 Possibilities of configurations in terms of fault occurrence. (a) Prefault system. (b) Post-fault system with fault at the rectifier B. (c) Post-fault system with fault at the rectifier A. (d) Post-fault system with fault at the inverter.

This way, four possibilities of configurations have been considered in terms of faults:

- 1) pre-fault ("healthy") operation
- 2) post-fault operation with fault at the rectifierB
- 3) post-fault operation with fault at the rectifierA
- 4) post-fault operation with fault at the inverter

Table 1 Efficiency of the proposed system normalized in terms conventional one

Frequency/Inductor	$(\eta_p/\eta_c - 1)$		
	S-Ca $\mu=0.5$	D-Ca $\mu=0.5$	D-Ca $\mu=0$
10kHz($i_g=i_g$)	-1.60%	-1.47%	-0.41%
10kHz($i_g=i_g/2$)	3.12%	3.25%	4.36%
5kHz($i_g=i_g$)	-0.74%	-0.27%	1.72%

When the fault occurrence is detected and identified by the control system, the proposed system is reconfigured and becomes similar to that in Fig.1. For instance, if a fault in any switch of rectifier A has been detected by the control system, the whole rectifier needs to be isolated. This isolation procedure depends on the kind of fault detected. If an open-circuit failure is detected, the control system will open all switches of the rectifier A. On the other hand, if a short circuit is detected, the control system will turn on all switches related to rectifier A, and in this case, the fuses will open, and consequently, the rectifier will be isolated, as discussed. Considering now a fault in one leg of inverter, in this case the SCR related with this leg is turned on and the leg *b1* is isolated, so that the leg *b2* of rectifier B will operate as the leg of inverter.

VII. MATLAB SIMULINK MODELS

The simulink models of the Proposed converter system, its control strategy and fault diagnosis is also carried out.

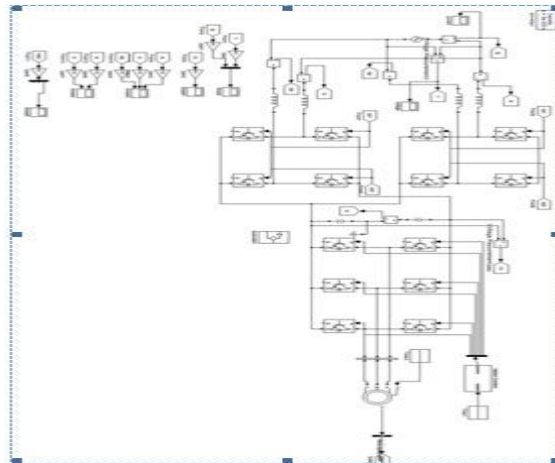


Fig 6 Simulink diagram of single phase to three phase drive system using two parallel single phase rectifiers

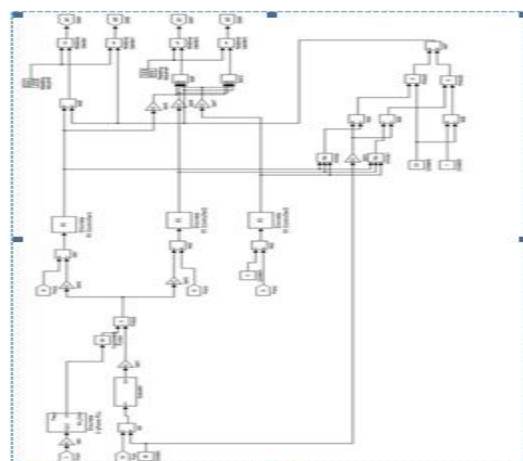


Fig 7 Sub-system

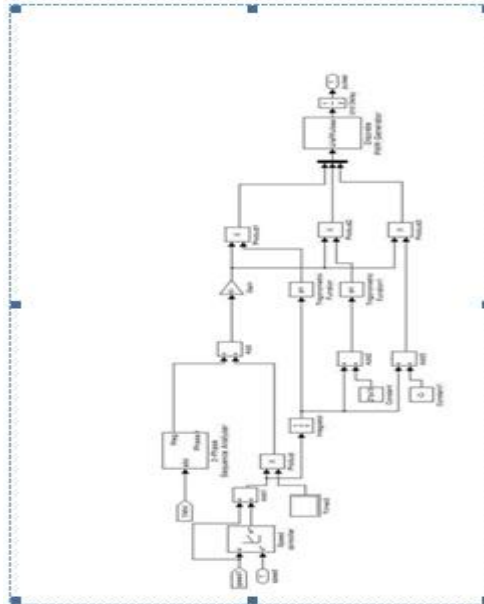


Fig 8 Vector control

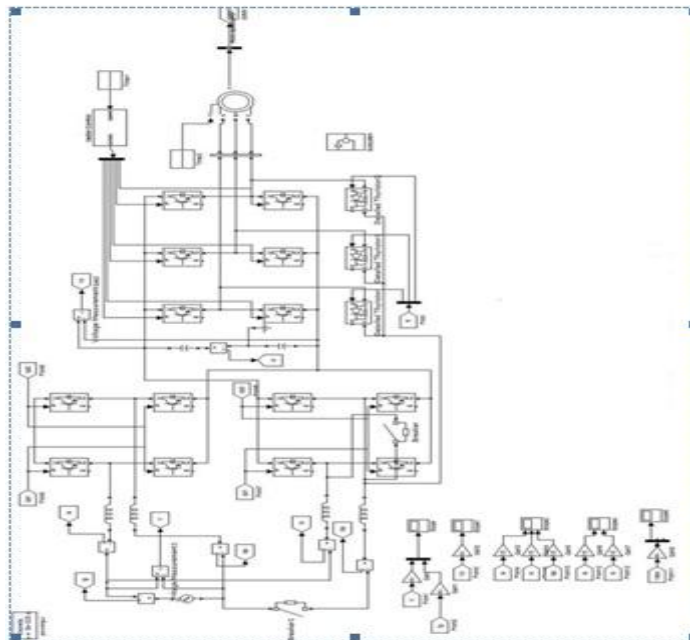
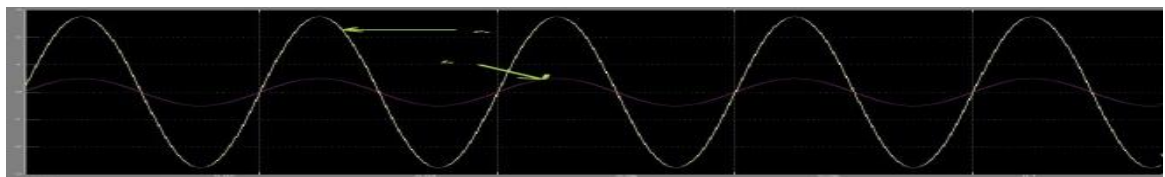
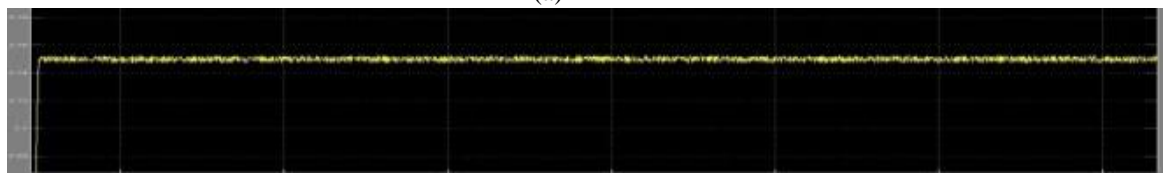


Fig 9 Fault Identification at Rectifier B

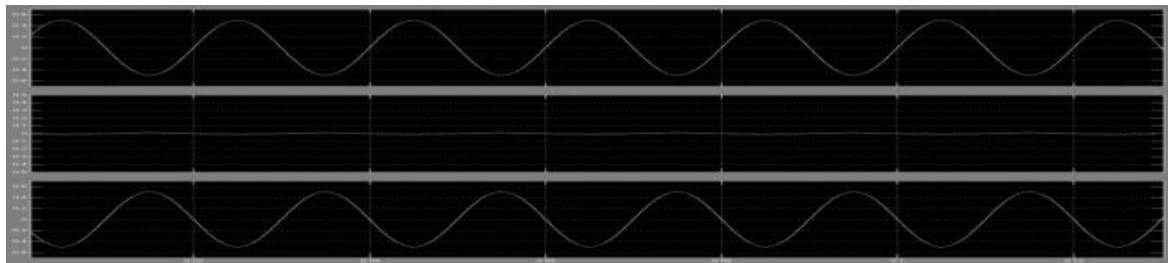
VIII. RESULTS



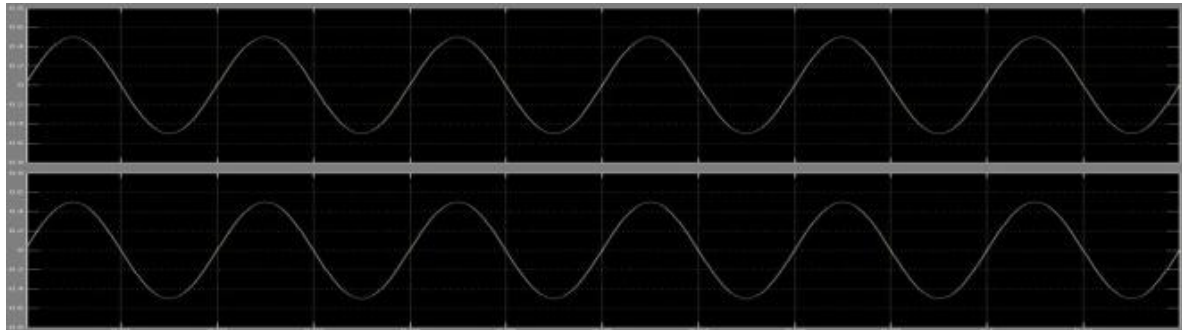
(a)



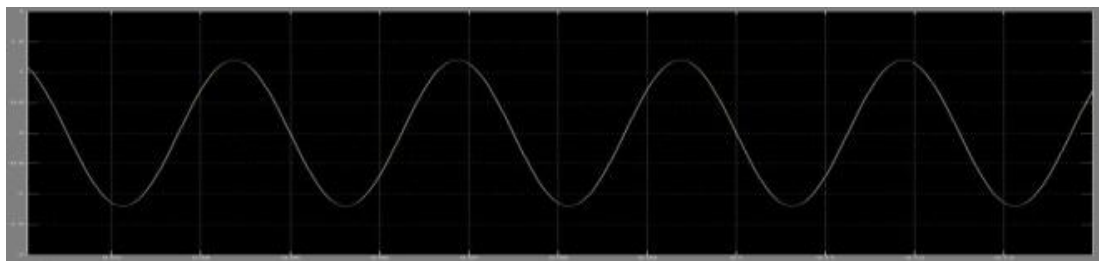
(b)



(c)

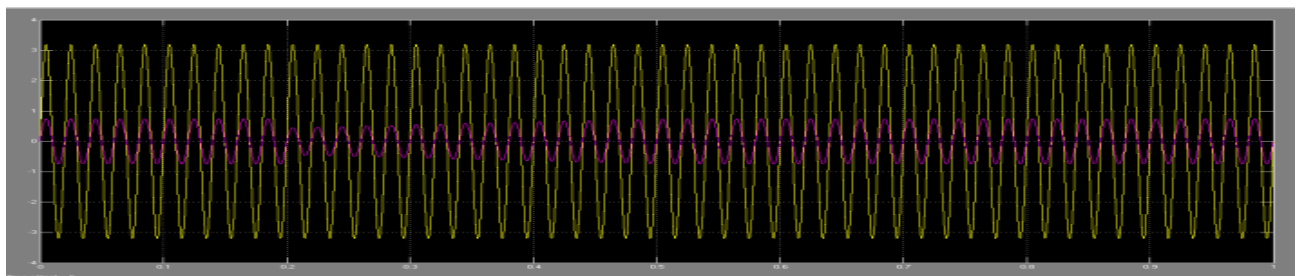


(d)

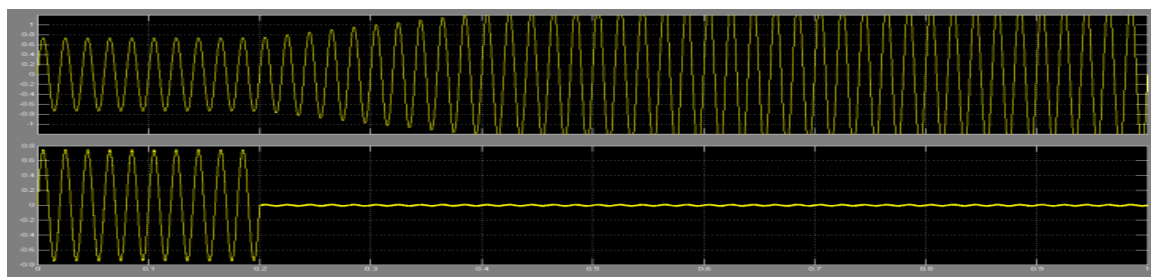


(e)

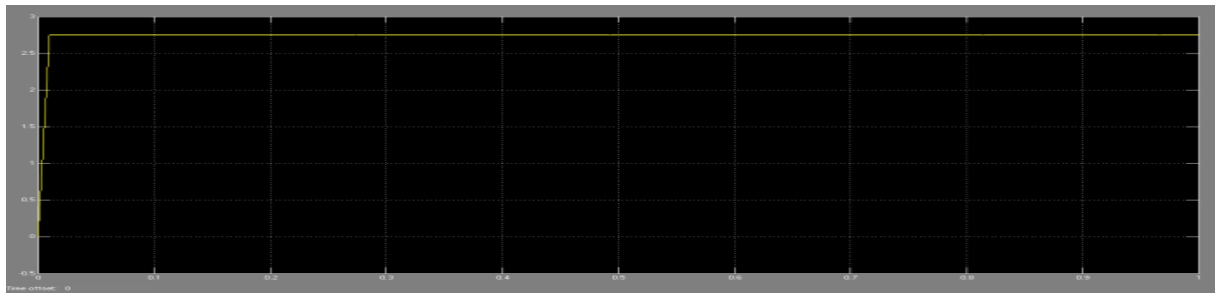
Fig. 10 Shows the waveforms of steady state three phase motor: (a) voltage and current of the grid, (b) dc-link voltage, (c) currents of rectifier A and circulating current, (d) currents of rectifiers A and B, and (e) load line voltage.



(a)



(b)



(C)

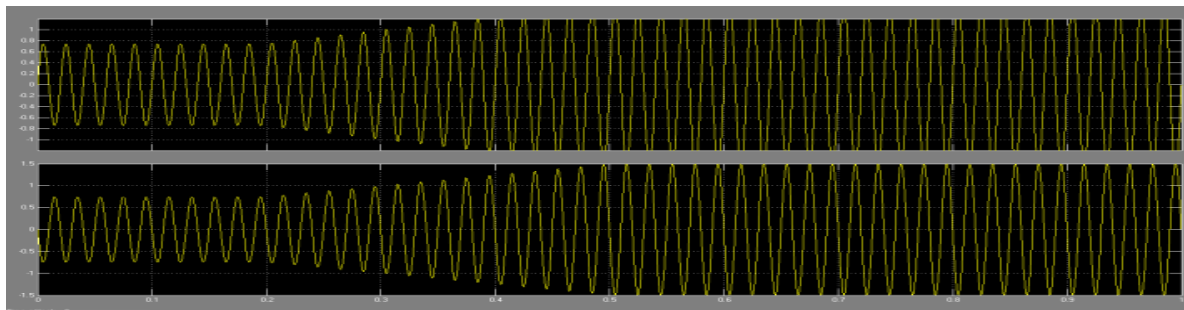


Fig 11 Experimental results when fault occurs at rectifier B. (a) Grid voltage and grid current

(b) Currents of rectifiers A and B (c) Capacitor voltage (d) Currents of rectifier A

IX. CONCLUSION

A single phase to three phase drive system using two parallel converters, three phase inverter and induction motor are proposed. The comparison between conventional and proposed system has been carried out and experimental results are also shown.

REFERENCES

- [1] P. Enjeti and A. Rahman, "A new single phase to three phase converter with active input current shaping for low cost AC motor drives," *IEEE Trans. Ind. Appl.*, vol. 29, no. 2, pp. 806–813, Jul./Aug. 1993.
- [2] B.K. Lee, B. Fahimi, and M. Ehsani, "Overview of reduced parts converter topologies for AC motor drives," in *Proc. IEEE PESC*, 2001, pp. 2019–2024.
- [3] C. B. Jacobina, M. B. de R. Correa, A. M. N. Lima, and E. R. C. da Silva, "AC motor drive systems with a reduced switch count converter," *IEEE Trans. Ind. Appl.*, vol. 39, no. 5, pp. 1333–1342, Sep./Oct. 2003.
- [4] C. B. Jacobina, E. C. dos Santos Jr., E. R. C. da Silva, M. B. R. Correa, A. M. N. Lima, and T. M. Oliveira, "Reduced switch count multiple three-phase machine drive systems," *IEEE Trans. Power Electron.*, vol. 23, no. 2, pp. 966–976, Mar. 2008.
- [5] D.-C. Lee and Y.-S. Kim, "Control of single-phase-to-three-phase AC/DC/AC PWM converters for induction motor drives," *IEEE Trans. Ind. Electron.*, vol. 54, no. 2, pp. 797–804, Apr. 2007.
- [6] L. Woo-Cheol, L. Taeck-Kie, and H. Dong-Seok, "A three-phase parallel active power filter operating with PCC voltage compensation with consideration for an unbalanced load," *IEEE Trans. Power Electron.*, vol. 17, no. 5, pp. 807–814, Sep. 2002.
- [7] L. Asiminoaei, E. Aeloiza, P. N. Enjeti, F. Blaabjerg, and G. Danfoss, "Shunt active-power-filter topology based on parallel interleaved inverters," *IEEE Trans. Ind. Electron.*, vol. 55, no. 3, pp. 1175–1189, Mar. 2008.
- [8] M. Ashari, W. L. Keerthipala, and C. V. Nayar, "A single phase parallel connected uninterruptible power supply/demand side management system," *IEEE Trans. Energy Convers.*, vol. 15, no. 1, pp. 97–102, Mar. 2000.
- [9] J.-K. Park, J.-M. Kwon, E.-H. Kim, and B.-H. Kwon, "High-performance transformer less online UPS," *IEEE Trans. Ind. Electron.*, vol. 55, no. 8, pp. 2943–2953, Aug. 2008.
- [10] Z. Ye, D. Boroyevich, J.-Y. Choi, and F. C. Lee, "Control of circulating current in two parallel three-phase boost rectifiers," *IEEE Trans. Power Electron.*, vol. 17, no. 5, pp. 609–615, Sep. 2002.
- [11] S. K. Mazumder, "Continuous and discrete variable-structure controls for parallel three-phase boost rectifier," *IEEE Trans. Ind. Electron.*, vol. 52, no. 2, pp. 340–354, Apr. 2005.
- [12] Z. Ye, P. Jain, and P. Sen, "Circulating current minimization in high frequency AC power distribution architecture with multiple inverter modules operated in parallel," *IEEE Trans. Ind. Electron.*, vol. 54, no. 5, pp. 2673–2687, Oct. 2007.
- [13] J. Holtz, "Pulse width modulation for electronic power conversion," *Proc. IEEE*, vol. 82, no. 8, pp. 1194–1214, Aug. 1994.
- [14] M. P. Kazmierkowski and L. Malesani, "Current control techniques for three-phase voltage-source PWM converters: A survey," *IEEE Trans. Ind. Electron.*, vol. 45, no. 5, pp. 691–703, Oct. 1998.
- [15] B. A. Welchko, T. A. Lipo, T. M. Jahns, and S. E. Schulz, "Fault tolerant three-phase AC motor drive topologies: A comparison of features, cost, and limitations," *IEEE Trans. Power Electron.*, vol. 19, no. 4, pp. 1108–1116, Jul. 2004.